Received: 20 January 2023 | Revised: 28 February 2023 | Accepted: 8 March 2023

DOI: 10.1002/agt2.339

Aggregate Open Access WILEY

REVIEW

A review of metal nanoparticle-based surface-enhanced Raman scattering substrates for severe acute respiratory syndrome coronavirus 2 (SARS-CoV-2) detection

Special Collection: Distinguished Australian Researchers

Norhayati Abu Bakar[1,2] | **Nur Nazhifah Yusoff**[2] | **Farah Shahadah Nor Azmi**[2] | **Joseph George Shapter**[1]

[1]Australian Institute for Bioengineering and Nanotechnology, University of Queensland, St Lucia, Australia

[2]Institute of Microengineering and Nanoelectronics, Universiti Kebangsaan Malaysia, Bangi, Malaysia

Correspondence
Joseph George Shapter and Norhayati Abu Bakar, Australian Institute for Bioengineering and Nanotechnology (AIBN), University of Queensland, 4067 St Lucia, Brisbane, Australia.
Email: j.shapter@uq.edu.au and norhayati.ab@ukm.edu.my

Funding information
Australian Research Council (ARC), Grant/Award Number: DP200101217

Abstract
Monitoring an infectious disease early using highly sensitive and non-invasive techniques is critical for human health. Interestingly, the development of surface-enhanced Raman scattering (SERS) for biological detection ideally fits these medical requirements and is rapidly growing as a powerful diagnostic tool. SERS can enhance the Raman signal of the target molecule by more than 10^6 after the adsorption of the molecule on the plasmonic nanostructured surface. This review provides an overview of the use of gold and silver nanoparticles in SERS substrate designs, followed by the development of these SERS substrates in severe acute respiratory syndrome coronavirus 2 (SARS-CoV-2) detection.

KEYWORDS
gold nanostars, SARS-CoV-2, SERS, silver nanostars

1 | INTRODUCTION

Surface-enhanced Raman scattering (SERS), a surface-sensitive method, enhances Raman scattering by adsorbing molecules on rough metal surfaces or nanostructures. In general, SERS enhancements are due to one of two mechanisms; namely electromagnetic mechanism (EM) or chemical mechanism (CM).[1–5] Surface plasmon excitation of noble metals increases the surface electromagnetic field in the EM mechanism, whereas in the CM mechanism charge transfer between the target molecules and substrate is involved.[6] Therefore, to provide the best signal enhancement, it is essential to have a substrate that can support both mechanisms. Common nanostructures used are based on gold and silver due to their unique localized surface plasmon resonance properties that can lead to strong enhancement for very sensitive detection at ultralow concentrations of molecules. These materials are also biocompatible and reliable for the analysis of biological species. The successful detection of analytes in biomedical analysis and imaging using SERS is influenced by metal nanoparticle materials, the nanoparticles' geometry, and the SERS substrate platform.

At its core, nanotechnology is the use of nanoscale materials for useful applications.[7] These materials can be 0-dimensional (e.g. nanoparticles), 1-dimensional (e.g. nanotubes), or 2-dimensional (e.g., graphene and many other monoatomic and "molecular" based sheets). This article will concentrate on the use of nanoparticles, in particular gold and silver, for application in developing SERS substrates for analysis of molecular or biological species.

Nanoparticles have evolved dramatically over the past 40 years. Initially, nanoparticles were strictly spherical with diameters below 100 nm. Recent efforts have seen shapes such as rods, triangles, cubes, and stars reported. The extensive efforts to make new shapes have been driven by various optoelectronic, antimicrobial, and catalytic applications among others.[8,9] In the case of SERS, sharp points are needed to generate the electric field enhancements required. This means spheres would likely not be as useful but the other shapes with sharp edges or points might be ideal platforms.

1.1 | Production of silver and gold nanoparticles

1.1.1 | Silver nanoparticle production

Spherical nanoparticles can be produced with a wide variety of methods[10] including many methods based on chemical

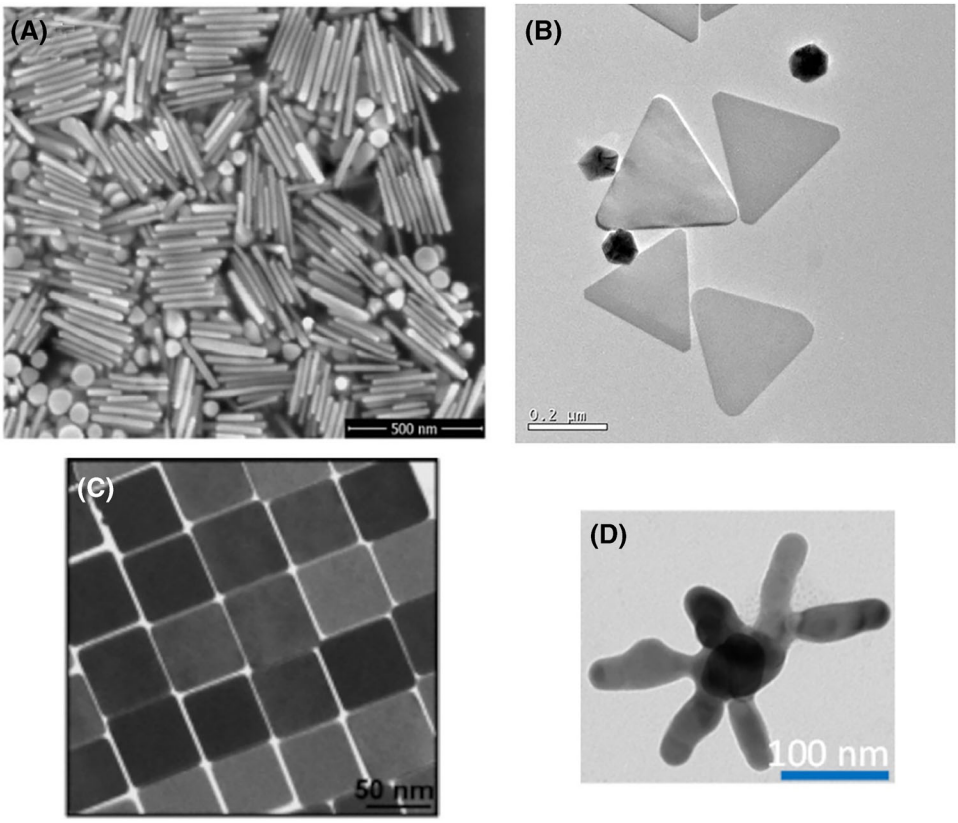

FIGURE 1 (A) FE-SEM image of silver nanorods. Reproduced with permission: 2018, Elsevier[15] (B) TEM image silver of nanotriangles. Reproduced with permission: 2015, Springer[21] (C) TEM images of Ag nanocubes. Reproduced with permission: 2004, American Chemical Society[108] (D) TEM image of silver nanostars. Unpublished Data.

reduction using different reducing agents[9] as well as various physical methods including arc discharge and photochemical methods using various types of radiation.[11] The chemical methods generally yield higher concentrations of nanoparticles but those particles are capped with a stabilizing agent while the physical approaches do not generally require capping agents.[12] There has been considerable work to use various natural agents like plants or biological species to make silver nanoparticles (AgNPs). These approaches work but typically do not yield nanoparticle dispersions of the same quality as chemical methods.[13,14]

Nanorods

Silver nanorods (AgNRs) can be synthesized using techniques such as seed-mediated growth, and photochemical and electrochemical approaches.[15] The seed-mediated synthesis is a solution-based method that uses standard approaches to make the silver seed metallic nanoparticles and growth solutions with capping agents (for example, cetyltrimethylammonium bromide [CTAB]) and reducing agents (for example, ascorbic acid [AA]) to make the rods. Control of the ratio of reagents means the aspect ratio of the rods can be controlled. Figure 1A shows a typical sample of silver nanorods.

Nanotriangles

Silver nanotriangles (AgNTs) are usually prepared with a seeding method.[16–19] A typical approach uses the dispersion of the initial nanoparticles with the addition of silver nitrate ($AgNO_3$) to polyvinylpyrrolidone (PVP) and AA (0.1 M) to produce the nanotriangles. The edge length of silver nanotriangles can be tuned by controlling the ratio of the capping agent (PVP), the $AgNO_3$,[16] and the amount of seed dispersion used.[20,21] Figure 1B shows a typical sample of silver nanorods.

Nanocubes

Silver nanocubes (AgNCs) have been produced in high concentrations via reduction by ethylene glycol in PVP because PVP preferentially binds to the Ag(100) face as opposed to the Ag(111) surface to promote the growth of a cubic structure.[22] Other approaches have used CTAB as a capping agent with glucose as a reducing agent.[23] Another method forms AgCl octahedra by mixing CF_3COOAg with cetyltrimethylammonium chloride which is then used to make the nanocubes using AA and $FeCl_3$.[24] Physical methods have used microwave heating in the presence of a polyelectrolyte to produce the nanocubes. Control of the cube dimensions is generally achieved by careful control of the conditions and concentration of the reagents involved. Figure 1C shows a typical sample of silver nanocubes.

Nanostars

The first reports of silver nanostars (AgNSs) used chemical reduction of Ag^+ in two steps with neutral hydroxylamine (HA) in the first reduction stage and citrate (CIT) in the second step.[25] A more recent report just used CIT as the reducing agent combined with microwave heating.[26] The AgNS produced via this approach have a very different morphology. Figure 1D shows a typical sample of AgNS.

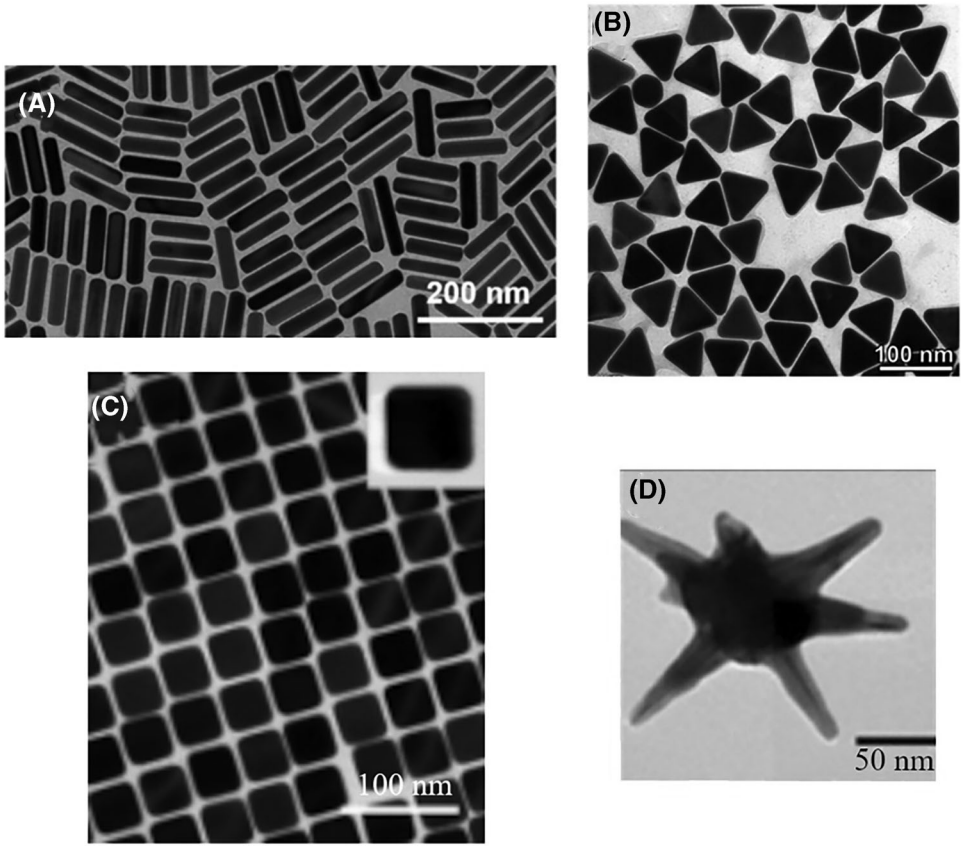

FIGURE 2 (A) TEM image of the AuNRs synthesized at low concentrations of CTAB. Reproduced with permission: 2021, American Chemical Society[33] (B) TEM image of horizontally oriented AuNTs. Reproduced with permission: 2018, American Chemical Society[36] (C) TEM image of refined AuNCs. Reproduced with permission: 2018, American Chemical Society[37] (D) TEM image of gold nanostars. Reproduced with permission: 2022, Wiley-VCH GmbH (European Chemical Societies Publishing).[41]

1.1.2 | Gold nanoparticle production

For gold nanoparticles, again the preparation methods can be separated into chemical (sometimes called bottom-up) and physical methods (top-down).[7,27] The chemical methods use reducing agents to obtain metallic gold from ions in concert with capping agents to stabilize the particles. In parallel to the approaches for silver, the physical methods typically break up bulk material with the application of energy often applied with light or ions. Various biological approaches have also been reported.[28]

Nanorods

There are three main methods to make gold nanorods (AuNRs). The first approach involved the growth of rods in templated pores on surfaces.[29] Another approach is based on electrochemical methods using a gold anode which is consumed and deposited on a cathode and subsequently removed into a dispersion.[30] The most common current method is seed-mediated growth which starts with a spherical nanoparticle and then through control of growth conditions sees the production of nanorods of various aspect ratios.[31–33] Figure 2A shows a typical sample of gold nanorods.

Nanotriangles

There are generally two approaches to growing gold nanotriangles (AuNTs). The first approach used vesicles in concert with polymers that act as both a capping agent to control the shape and the reducing agent.[34] The particles produced in this approach are very high quality and can have a high dispersity. The second approach is the typical seed-mediated approach with two growth steps. The addition of iodide ions has been shown to improve the obtained AuNTs.[35] A seedless approach uses 3-butenoic acid as the reducing agent in the presence of benzyldimethylammonium chloride as a capping agent. With heating, this method can produce larger nanotriangles.[36] Figure 2B shows a typical sample of AuNTs.

Nanocubes

The best gold nanocubes (AuNCs) have been synthesized with a seed-mediated method using 10 nm nanoparticles followed by the introduction of bromide ions and gold (III) chloride trihydrate ($HAuCl_4$) with AA as the reducing agent.[37] Surface-mediated production of gold nanocubes uses templated and polymers to control the cube size.[38] Biological-based synthesis of gold nanocubes has also been reported although the quality of the cubes is not as high.[39] Figure 2C shows a typical sample of gold nanocubes.

Nanostars

Gold nanostars (AuNSs) were first reported in high yield using a seeding approach through the reduction of $HAuCl_4$ in a concentrated solution of PVP in DMF.[40] A seedless approach using 4-(2-hydroxyethyl)-1-piperazineethanesulfonic acid has been developed although a capping agent is still required to stabilize the dispersion.[41,42] These seedless approaches usually have

much broader dispersions of nanostars in terms of their sizes and shape. Recent efforts have produced the AuNS using reducing agents coupled with charged surfactants to produce micelles.[43] Figure 2D shows a typical sample of AuNS.

1.1.3 | Combination of gold and silver for SERS

There has been considerable work highlighting that using gold and silver together can give enhanced SERS performance. Gold nanorods with a coating of silver improved the figure of merit for SERS detection by up to a factor of 5.[44] In the case of nanocubes, coating gold nanocubes with silver can yield signals up to six times larger than bare cubes.[45] For nanostars, gold has been used as the base material with a coating of silver to yield increases in the SERS intensity again by about a factor of 5.[46] AgNS have also been adsorbed to gold nanorods which provides a SERS enhancement of about 10.[47]

2 | USE OF GOLD AND SILVER AS SERS SUBSTRATES

SERS substrates have been studied to achieve powerful spectroscopic devices able to detect and identify trace amounts of chemicals based on their unique vibrational characteristics, especially in complex matrices. The fabrication of simple, reproducible, reusable, reliable, and stable SERS substrates is still the most important factor for the development of powerful SERS substrates.[48] The SERS substrate plays a critical role as the Raman signal amplifier for the target molecule after absorption on the plasmonic nanostructured surface. The SERS substrate is typically designed to operate in the visible or near-infrared range at 400–1000 nm because the SERS enhancements are strongly wavelength dependent.[49] Therefore, the common metal nanoparticles used in SERS are gold and silver because of their unique optical properties to give good plasmon resonance for SERS using excitation wavelengths from 400–1000 nm. Gold has been the most used metallic material because it is more easily stabilized by chemical means and more stable from oxidation than silver colloids. Interestingly, gold is very well known for its biocompatibility and bioinert properties that are suitable for interactions with living tissues.[50]

However, silver colloids are still applied extensively for SERS even though silver colloids have less stability than gold colloids. Silver still has a sufficiently long shelf-life after its preparation in the laboratory and becomes more stable after deposition on a solid surface to produce a SERS substrate. Silver particles were first discovered as SERS materials and also reported to have a larger electromagnetic enhancement in the visible range ensuring high sensitivity in SERS detection.[51] The other important SERS substrate parameter is larger surface areas to maximize analyte adsorption thus providing the maximum number of molecules producing the signal. This parameter must be considered during the fabrication of the SERS substrate platform in applications. Normally SERS substrates will be prepared in one of two types of platforms – namely solution-based SERS or solid-based SERS. Here, we will discuss these two types of SERS platforms that use gold and silver as the SERS active element.

2.1 | Solution-based SERS

Solution-based SERS typically uses a colloidal SERS material. This technique has been widespread and used in SERS for almost 35 years and the knowledge has been accumulated in various fields. Researchers use this colloidal platform in SERS applications due to its simplicity, low cost, and accessibility for SERS detection rather than a solid-SERS substrate. Commonly this colloidal gold and silver can be mixed directly with the analytes in a cuvette for the SERS measurements.[52–57] The preparation of gold and silver can be done easily in the laboratory by tailoring the nanoparticle size and geometry before mixing them with the analytes. Using this colloidal approach, researchers can tailor single or multiple numbers of nanoparticles to interact with the analyte before SERS measurement. An interesting study by the Ma group to detect metal ions tuned the size of gold nanostars dimer before injecting the metal ions into the nanostars solution.[58]

Colloidal metal nanoparticles can be mixed with a cellulose solution for lightweight and flexible support before the adsorption of the detected molecule.[59] However, colloidal dispersions can have an issue with nanoparticle aggregation and have a very high tendency for over-aggregation in solution which can lead to no hotspot area and no plasmonic activity.[56] At the same time, analyte detection is limited due to solubility during the direct mixing of the analyte solution and colloidal nanoparticle. In order to increase the sensitivity and reproducibility of SERS substrates, researchers have explored alternative platforms by employing various approaches to assembling nanoparticles onto different solid surfaces.

2.2 | Solid-based SERS

Solid-based SERS normally use one of two approaches – namely electrochemically roughened electrodes or planar substrates using either non-lithography or lithography fabrication. The electrochemically roughened electrode approach has been used since the discovery of Raman scattering enhancement of pyridine on silver electrode metal surfaces by Fleischmann, Hendra, and McQuillan in 1974.[60] SERS using solid support is straightforward and usually done either by depositing the analyte solution on the electrode surface or immersing the electrode in the analyte solution after the gold or silver electrode surface was roughened in the solution.[61,62] This mixture also can be dried on the surface to assist the molecular adsorption to the nanoparticle interface which can generate higher SERS intensity. The Lin group dried a solution mixture of colloidal gold nanostars and paraquat solution on the gold-coated slide to increase surface area and substrate-analyte interactions.[63] This platform proved that monitoring paraquat residue in green tea samples using SERS is more facile than traditional testing techniques such as high-performance liquid chromatography and gas chromatography-mass spectroscopy.

Researchers have explored non-lithography and lithography fabrication for SERS substrates to yield nanoscale features and increase the non-uniform enhancement generated from the surface roughness of the electrode. The popular approach in non-lithography is assembling the nanoparticles on a solid substrate such as glass and silicon surface before depositing the molecule to be detected on the metal nanoparticle surface. This approach has been used both with and without a template to promote the metal nanostructures' adhesion on the solid surfaces.[16,64] The coverage and nanoparticles arrangement on the solid surface can be easily controlled which can help to generate homogenous SERS enhancement of the analyte molecules. Hydrothermal growth[65] and seed-mediated growth of nanoparticles[66] on the solid surface are alternative approaches that offer good controllable distribution of the active species on the SERS platform. The approaches are similar to electron beam lithography for controlling the size, shape, and separation of the nanoparticles.[67,68] However, non-lithography is more attractive to researchers in SERS substrate fabrication due to simple and low-cost procedures compared to the lithography processes. Easy transfer of the nanoparticles to the surface using common equipment and reagents in the laboratory makes non-lithography ideal for SERS substrate fabrication.

3 | SILVER NANOPARTICLES IN SARS-CoV-2 DETECTION

Silver is known to have antimicrobial activity against viruses, fungi, and bacteria. Owing to their selective toxicity against microorganisms and bacterial capacity,[69] AgNPs are long-established in biomedicine especially to fight off human pathogenic viruses such as a Respiratory syncytial virus, Influenza virus, Norovirus, Hepatitis B virus, and Human immunodeficiency virus.[70] Numerous studies have shown that AgNPs are able to attach to the cellular membrane, modifying the cell's respiratory functions and cellular permeability. It is likely that AgNPs penetrate the bacteria's membrane while interacting with the membrane surface.[71] Silver nanomaterials are commonly used in SERS biosensing thanks to their high electrical and thermal conductivity.[72–81] The size and morphology of Ag nanomaterials will determine the SERS properties.[82] The accuracy and sensitivity of detection depend on the structure's morphology. Several parameters such as surrounding temperature, electrolyte composition, electrodeposition time, and potential can be adjusted in order to get different morphology of Ag nanostructures.[83–85]

Recently, a study on different morphologies of Ag nanostructures on SERS performance to detect coronavirus disease 2019 (COVID-19) has been carried out. In this study, four Ag nanostructures namely dendritic, bulk, globular, and spiky, are formed by changing the parameters during the preparation of AgNPs (see Figure 3A). When a solution of the cationic dye Rhodamine 6G (R6G) is added to the AgNPs SERS substrate, dendritic Ag nanostructures were shown (see Figure 3A) to have Raman signal higher than the other three Ag nanostructures. This phenomenon is attributed to the coarse nanostructures and larger surface area of dendritic Ag nanostructures which improved the detection efficiency lowering the limit of detection. Based on these results, the dendritic Ag nanostructures were then chosen as a sensing medium for detecting SARS-CoV-2 RNA sequences. It is observed that the Raman signal increased progressively as the concentration of severe acute respiratory syndrome coronavirus 2 (SARS-CoV-2) increased, with a detection limit of 7.42×10^{-14} M.[86]

At high ionic strength, AgNPs tend to aggregate on virus particles as AgNPs interact strongly with virus surface proteins.[87,88] With increasing protein concentration, these aggregated AgNPs will subsequently create inhomogeneities of the electromagnetic field with high local density (hotspots) near the surfaces. Zavyalova et al. reported that SERS-aptasensor based on colloidal silver proved to be specific, rapid (7 min), simple (one step) and highly sensitive with limit of detection at 5.5×10^4 TCID50/mL (Median Tissue Culture Infectious Dose). It was discovered that more labelled aptamers accumulate to the target SARS-CoV-2 virion while fewer labelled aptamers formed on the controlled viruses of Influenza A virion for the same enhancement spot from AgNPs aggregates. This occurrence is due to aggregation of AgNPs on the virus particles which lead to more reporter molecules near SARS-CoV-2 and ultimately increasing the SERS signal as the concentration of SARS-CoV-2 increases. This results in an enhancement of SERS signal at higher concentration of SARS-CoV-2 (see Figure 3B).[89]

The spike glycoprotein of SARS-CoV-2 consists of an S1 subunit which has a receptor binding domain that recognizes the human receptor angiotensin-converting enzyme 2 (ACE2) for cell entry.[90,91] This binding specificity means that ACE2 can be used as an anchor to encapsulate SARS-CoV-2 from human or environmental samples. Zhang et al. conducted a study employing silver nanorods as SERS substrate for onsite cross-examination of SARS-CoV-2 in water. When spike protein is loaded onto ACE2@Ag nanorods-SERS substrate the spectra displayed a quenching of SERS signal intensity specifically at Raman shifts of 1089, 1189, and 1447 cm^{-1}. A red-shift from 1189 to 1182 cm^{-1} from vibrational of N-H bonding was observed and it is correlated to the enhancement of 1182 cm^{-1} from SARS-CoV-2 (see Figure 3C). This is possibly caused by the change in N-H vibration mode or N-H bond length[92,93] which happens when the H-bond of the ACE2 is interfered with after recognizing SARS-CoV-2 spike protein. No Raman shift from 1189 to 1182 cm^{-1} is observed when *E. coli*, extracted proteins of *E. coli* and bacteriophage Phi6 are loaded onto ACE2@Ag nanorods-SERS substrate. Zhang and team also collected water samples from wastewater at Huanan Seafood Market, the suspected first place of COVID-19 outbreak in China. The wastewater samples give positive RT-qPCR test (2.88×10^4 copies/L). The 1182/1189 cm^{-1} ratios and a principle component analysis approach showed that SARS-CoV-2 can be traced at the pipeline entry (see Figure 3C). This fabricated ACE2@Ag nanorods-SERS assay is crucial as it provides onsite detection of SARS-CoV-2 with a portable Raman spectrometer, compared to an RT-qPCR assay in which RNA extraction and laboratory amplification is necessary to carry out the test. These outcomes indicated that Ag nanorods-SERS substrate bound with ACE2 was able to recognize SARS-CoV-2 spike proteins and consequently changed the ACE2 structures to induce SERS signal quenching.[94]

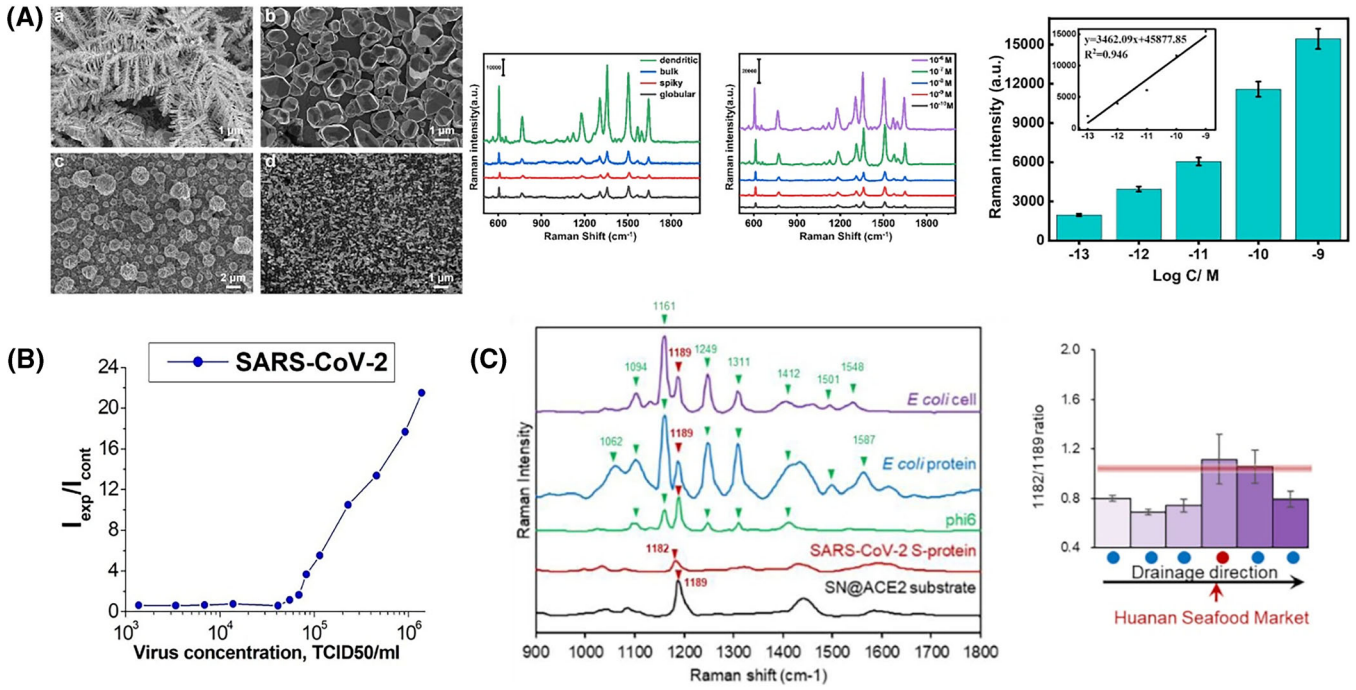

FIGURE 3 (A) SEM images of the silver nanostructures at different electrochemical conditions; dendritic (a), bulk (b), globular (c), and spiky (d) Ag nanostructures with corresponding Rhodamine 6G (R6G) SERS intensity with different Ag structures and concentration-dependent spectra and calibration curve from the dendritic surface. Reproduced with permission: 2022, Elsevier[86] (B) Concentration curve for SARS-CoV-2 from SERS spectra from Ag nanoparticles. Reproduced with permission: 2021, MDPI[89] (C) Comparison of SERS signals between SARS-CoV-2 spike protein and other bacteria on the Ag nanorod substrate. Only SARS-CoV-2 spike protein represents the Raman shift from 1189 to 1182 cm^{-1}. Applications of on-site SERS interrogation for SARS-CoV-2. Change of 1182/1189 ratio in the pipeline of Huanan Seafood Market. Red and blue dots indicated water samples with positive and negative qPCR results for SARS-CoV-2. Reproduced with permission: 2021, Elsevier.[94]

4 | GOLD NANOPARTICLES IN SARS-COV-2 DETECTION

Gold nanostars have been used as a material in biosensors for the detection of SARS-CoV-2 viral RNA or their proteins (Spike, Envelope, Membrane, and Nucleocapsid). The structure of the gold nanostars is beneficial for chemical interaction with the virus. There are several types of sensors using gold nanostars as the main material in COVID-19 detection such as nanoparticle surface energy transfer spectroscopy, surface-enhanced Raman spectroscopy, and electrochemical-based sensors. Table 1 shows the summary of SERS-based sensors that used gold nanoparticles for COVID-19 detection. In this section, studies involving gold nanoparticle synthesis and its application for SARS-CoV-2 detection will be discussed.

Pramanik et al.[95] prepared dye R6G conjugated DNA aptamer conjugated gold nanostars for detection of the SARS-CoV-2 spike recombinant antigen or SARS-CoV-2 spike protein pseudo typed baculovirus by nanoparticle surface energy transfer (NSET) spectroscopy. Aptamers are short, single-stranded oligonucleotides (DNA or RNA) that bind to targets with high affinity and specificity by folding into tertiary structures.[96] Aptamers have been extensively used in basic research to ensure food safety and monitor the environment. Aptamers have several advantages such as shorter generation time, lower cost of manufacturing, no batch-to-batch variability, higher modifiability, better thermal stability, and higher target potential. In this work, the NSET is governed by the distance between the dye and the gold nanoparticle surface. The presence of the SARS-CoV-2 spike recombinant antigen leads to binding with aptamer pushing the dye away from the nanoparticle. Figure 4A) shows the reduction in the SERS intensity in the presence of the antigen proving the effect of the binding. The authors use this effect to measure the dye fluorescence in the presence of the varying amounts of antigen and show a limit of detection (LOD) of the antigen of 130 fg/mL. A similar approach was used by Bistaffa et al. using methylene blue as the SERS reporter molecule and COVID-19 spike protein antibodies as the binding mechanism.[97] A LOD of 0.046 ng/mL (0.60 pM) was demonstrated.

Sanchez et al.[98] selected gold nanostar nanoparticles and MoS_2 thin layers as a material for COVID-19 virus detection by using surface-enhanced Raman spectroscopy (SERS). The advantage of this approach is that it uses a straight interaction between the nanostars and the COVID-19 structures. They detected the SARS-CoV-2 virion particles, its spike (S) and nucleocapsid proteins (N). The method to produce gold nanostars in this work incorporates addition of copper atoms. This method was proposed by Jose-Yacaman and his team where they controlled selective growth and high-yield production of $Au_{rich}Cu$ concave pentagonal nanoparticles ($CPNP_s$) and their evolution into branched nanostructures via seed mediated growth by using oleylamine as a capping and self-assembly promoter agent. Addition of Cu produces a 5-arm structure with concave facets and sharp tip surface. Figure 4B) shows the SEM image of the Au-Cu nanostars used as SERS substrates. The image shows very sharp points which can enhance the Raman signal. By using Raman-SERS spectroscopy, the structure of the proteins and in situ changes produced by different conditions can be followed. As shown

TABLE 1 SERS-based sensors for the diagnosis of SARS-CoV-2

Sensor type	Sensor configuration/ Laser Wavelength (nm)	Recognition element (SARS-CoV-2)	Analytical sensitivity	Limit of Detection	References
Nanoparticle Surface Energy Transfer Spectroscopy	Aptamer conjugated gold nanostar/532	Spike protein and virus particles	10–500 virus/mL	130 fg/mL (spike protein), 8 virus/mL	[95]
Surface-enhanced Raman spectroscopy	Antibody conjugated gold nanoparticles/633	Spike protein	0.01–100 ng/mL	0.046 ng/mL (0.60 pM)	[97]
Surface-enhanced Raman spectroscopy	Gold-copper nanostars/785	Spike and nucleocapsid protein	744 μM–7 nM	8.89×10^{-9} M	[98]
Surface-enhanced Raman spectroscopy	Hollow gold nanostars/633	SARS-CoV-2 lysate	0–10^4 PFU/mL	5.1 PFU/mL	[99]
Surface-enhanced Raman spectroscopy	DNA conjugated gold nanoparticles/633	Viral RNA	10^{-8}–10^{-14} M of RNA	395 fM	[100]
Surface-enhanced Raman spectroscopy	Antibody conjugated gold nanoparticles and magnetic beads/633	SARS-CoV-2 antigen and lysate	0.01–100 pg/mL for antigen and 5–1000 PFU/mL for lysate	2.56 fg/mL for antigen and 3.4 PFU/mL for lysate	[101]
Surface-enhanced Raman spectroscopy	Antibody conjugated gold nanoparticles and magnetic beads/785	Spike Protein and Virus	10–10^7 fg/mL for spike protein and 1.3×10^3–1.3×10^9 genomes/mL for the virus	257 fg/mL for spike protein and 4.1×10^4 genomes/Ml for the virus	[102]

in Figure 4B), the analytical sensitivity in this work for the spike protein ranged from 744 μM to 7 nM while the LOD was 8.89×10^{-9} M.

Yu et al. tried several nanoparticle structures including hollow gold nanostars as SERS substrates for SARS-CoV-2 detection.[99] Hollow gold nanoparticles were synthesized first followed by star-shaped hollow gold nanostars through gold seeding process. Figure 4C) shows the schematic illustration of the synthetic process for hollow Au nanostars (HAuNSs). Hollow gold nanostars shows a substantial localized surface plasmon effect at the single-particle level and good stability under saline conditions compared to gold nanoparticles but it is hard to control the aggregation of the particles. Besides, it also difficult to create hot spots as gold nanoparticles cannot develop hot spots at the single-particle level. The nanostars were modified with antibodies for protein binding and BSA to prevent non-specific binding. The hollow gold nanostars as SERS substrates were able to detect a wide dynamic range of virus concentrations from 0 to 10^4 Plaque forming units (PFU)/mL and has a limit of detection of 5.1 PFU/mL as shown in Figure 4C). This was a greater sensitivity than the coresponding ELISA approach.

Gao et al. have also used SERS, in combination absorption and fluorescence to detect COVID-19 RNA using DNA modified gold nanoparticles.[100] The limit of detection for the SERS approach was 395 fM which was slightly higher than the other approaches used to reinforce the measurements. One of goals in work related to sensing of COVID-19 has to be real world, rapid and sensitive testing of patients with approaches that require little to no sample processing. Cha et al. using a combination of antibody modified hollow gold nanoparticles with an MGITC reporter attached in concert with antibody modifed magnetic beads to enhance collection efficiency were able to reliably detect COVID-19 from patient samples.[101] This assay had detection limits of 2.56 fg/mL for the SARS-CoV-2 antigen and 3.4 plaque-forming units/mL for the SARS-CoV-2 lysates. The diagnosis of COVID-19 from patients was done within 30 min using a portable Raman device (see Figure 4D). Antoine et al. used a very similar approach which could be used at point of care and detected several variants of the virus.[102]

A variety of other approaches to sensing SARS-CoV-2 have been reported.[103] Clearly, the most common sensors for SARS-CoV-2 are the at-home rapid antigen tests (RATs). They have the significant advantage of minimal required sample processing but it can take 3 to 7 days after infection for there to be enough virus to be detected by the test. Manufacturers report LODs ranging from tens to hundreds of TCID50/mL of virus although there are reports suggesting these sensitivities are much lower than the true values.[104] SERS-based RAT tests have recently been reported and these approaches have increased the sensitivity by a factor of about 100.[105] ELISA approaches have also been developed with LODs of about 100 PFU/mL which is about 30 times less sensitive than the SERS approaches developed in the same lab.[105] A field effect transistor (FET)-based biosensor has shown a LOD of 1 fg/mL of the spike protein in lab samples and 100 fg/mL in clinical samples. This sensor also was able to detect virus proteins at 1.6×10^1 PFU/mL.[106] Other approaches are using data from wearable sensors to measure health parameters and data processing to detect infection but these do not detect SARS-CoV-2.[107]

The future of COVID-19 detection will have to focus on two aspects; namely detection of the presence of the virus and the earliest possible detection of infection. These two steps will help minimize the spread of the virus to keep its impact as small as possible which will save many lives. Rapid, real-time, in situ monitoring of the environment will be key for the earliest detection of the presence of the virus. There are many examples of monitoring wastewater but the detection of biological species is not done in-line or real-time. The SERS sensors discussed here do present this opportunity but would likely require strategies to renew the substrate to maintain sensitivity. Other approaches to prevent infection in the first place include air monitoring which is now being

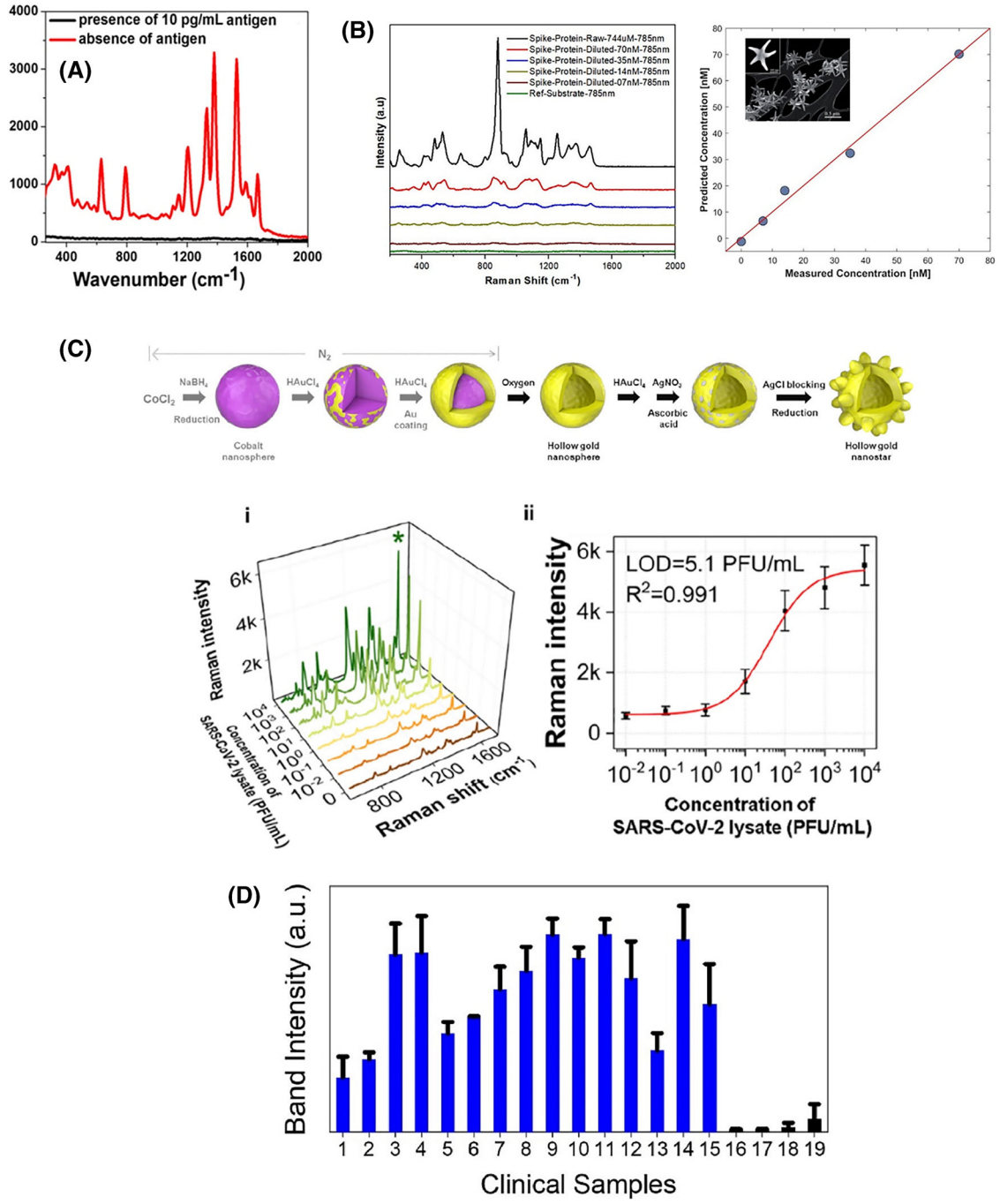

FIGURE 4 (A) Rhodamine 6G (R6G) SERS intensity reduction from COVID-19 antigen binding to DNA aptamer modified gold nanoparticle. Reproduced with permission: 2021, American Chemical Society[95] (B) SERS spectra of various concentrations of the COVID-19 spike protein and the calibration curve obtained using PLSR (Partial Least Squares Regression) with two principal components. Inset: SEM image of Au-Cu nanostars as the SERS substrate. Reproduced with permission: 2021, Royal Society of Chemistry[98] (C) Schematic illustration of the synthetic process of hollow Au nanostars; (i) SERS spectra for COVID-19 lysate and (ii) corresponding calibration curve in the range of 0–10^4 PFU/mL. Reproduced with permission: 2021, Wiley[99] (D) SERS detection of COVID-19 from real patients. Samples 1–15 were obtained from patients positively diagnosed with COVID-19, whereas samples 16–19 were from negatively diagnosed patients. Reproduced with permission: 2022, Elsevier.[101]

developed commercially. A SERS-based system will be ideal for these applications. SERS substrates that combine the use of gold and silver have been shown to have improved sensitivity and this could be explored for SARS-CoV-2 detection. In terms of the detection of infection, the current RAT tests have the right properties but lack sensitivity. SERS represents an opportunity to overcome this shortcoming as shown but work to address things like shelf life and reproducibility will need to be undertaken before commercial products can be launched.[105]

5 | CONCLUSION

COVID-19 is a highly contagious respiratory infection caused by the SARS-CoV-2 virus. Early detection of the SARS-CoV-2 virus in humans and animals using fast and accurate analytical methods can minimize the spread of this infectious disease. Fast and accurate diagnosis methods that have the ability to detect the virus at very low protein concentrations and without pre-treatment or in complex matrices are very important. The unique characteristics of SERS have

opened the door to future biological analysis with simple procedures adsorbing the SARS-CoV-2 spike protein on the metallic nanostructures to enhance sensitivity ensuring reliable testing even at the early stage of the infection. Significant advances in surface-enhanced Raman scattering techniques for the detection of SARS-CoV-2 are leading to diagnostic precision and make it a promising candidate for point-of-care testing. The design of SERS substrates and platforms in virus detection can lead to the successful identification of unique gene sequences and DNA based on their specific vibrational characteristic. Moreover, substrate fabrication is readily integrated into analytical systems for portable SERS analysis and can be integrated with other methods such as electrochemistry to increase the sensitivity in biomedical matrices without filtration and treatment before diagnosis.

ACKNOWLEDGMENTS

This work was supported by Australian Research Council (ARC) funding [DP200101217]. Norhayati Abu Bakar would like to thank the Ministry of Higher Education Malaysia and Universiti Kebangsaan Malaysia for her fellowship.

CONFLICT OF INTEREST STATEMENT

The authors declare no conflict of interest.

ORCID

Norhayati Abu Bakar https://orcid.org/0000-0002-8723-8745
Joseph George Shapter https://orcid.org/0000-0002-4000-2751

REFERENCES

1. Y. Zhang, Z. Wang, L. Wu, Y. Pei, P. Chen, Y. Cui, *Analyst* **2014**, *139*, 5148.
2. Y. S. Yamamoto, T. Itoh, *J. Raman Spectrosc.* **2016**, *47*, 78.
3. T. Itoh, Y. S. Yamamoto, Y. Ozaki, *Chem. Soc. Rev.* **2017**, *46*, 3904.
4. H. O. Chu, S. Song, C. Li, D. Gibson, *Coatings* **2017**, *7*, 26.
5. M. Xia, *Spectrosc. An Int. J.* **2018**, 4861472. https://doi.org/10.1155/2018/4861472
6. S. Uskoković-Marković, V. Kuntić, D. Bajuk-Bogdanović, I. Holclajtner-Antunović, *Encyclopedia of Spectroscopy and Spectrometry (Third Edition)* **2017**, 383. https://doi.org/10.1016/B978-0-12-409547-2.12163-8
7. S. J. Amina, B. Guo, *Int. J. Nanomed.* **2020**, *15*, 9823.
8. Z. Zhang, W. Shen, J. Xue, Y. Liu, Y. Liu, P. Yan, J. Liu, J. Tang, *Nanoscale Res. Lett.* **2018**, *13*, 54.
9. C. Quintero-Quiroz, N. Acevedo, J. Zapata-Giraldo, L. E. Botero, J. Quintero, D. Zárate-Triviño, J. Saldarriaga, V. Z. Pérez, *Biomater. Res.* **2019**, *23*, 27.
10. A. Almatroudi, Silver nanoparticles: synthesis, characterisation and biomedical applications *Open Life Sci*. **2020**, *15*, 819.
11. S. Iravani, H. Korbekandi, S. V Mirmohammadi, B. Zolfaghari, *Res. Pharm. Sci.* **2014**, *9*, 385.
12. X.-F. Zhang, Z.-G. Liu, W. Shen, S. Gurunathan, *Int. J. Mol. Sci.* **2016**, *17*, 1534.
13. E. Rodríguez-León, R. Iñiguez-Palomares, R. E. Navarro, R. Herrera-Urbina, J. Tánori, C. Iñiguez-Palomares, A. Maldonado, *Nanoscale Res. Lett.* **2013**, *8*, 318.
14. T. Liu, D. R. Baek, J. S. Kim, S.-W. Joo, J. K. Lim, *ACS Omega* **2020**, *5*, 16246.
15. C. R. Rekha, V. U. Nayar, K. G. Gopchandran, *J. Sci. Adv. Mater. Devices* **2018**, *3*, 196.
16. N. Bakar, J. Shapter, M. Salleh, A. Umar, *Appl. Sci.* **2015**, *5*, 209.
17. Y. Zhong, G. Liang, W. Jin, Z. Jian, Z. Wu, Q. Chen, Y. Cai, W. Zhang, *RSC Adv.* **2018**, *8*, 28934.
18. A. Amirjani, N. N. Koochak, D. F. Haghshenas, *Mater. Res. Express* **2019**, *6*, 036204.
19. G. Hu, W. Zhang, Y. Zhong, G. Liang, Q. Chen, W. Zhang, *Curr. Appl. Phys.* **2019**, *19*, 1187.
20. M. Gao, L. Sun, Z. Wang, Y. Zhao, *Mater. Sci. Eng. C* **2013**, *33*, 397.
21. C. Wu, X. Zhou, J. Wei, *Nanoscale Res. Lett.* **2015**, *10*, 354.
22. Z. Chen, T. Balankura, K. A. Fichthorn, R. M. Rioux, *ACS Nano* **2019**, *13*, 1849.
23. T. Jiang, B. Wang, L. Zhang, J. Zhou, *J. Alloys Compd.* **2015**, *632*, 140.
24. S. Zhou, J. Li, K. D. Gilroy, J. Tao, C. Zhu, X. Yang, X. Sun, Y. Xia, *ACS Nano* **2016**, *10*, 9861.
25. A. Garcia-Leis, J. V. Garcia-Ramos, S. Sanchez-Cortes, *J. Phys. Chem. C* **2013**, *117*, 7791.
26. R. N. Revnic, G. F. Știufiuc, V. Toma, A. Onaciu, A. Moldovan, A. B. Țigu, E. Fischer-Fodor, R. Tetean, E. Burzo, R. I. Știufiuc, *Int. J. Mol. Sci.* **2022**, 23.
27. S. Yazdani, A. Daneshkhah, A. Diwate, H. Patel, J. Smith, O. Reul, R. Cheng, A. Izadian, A. R. Hajrasouliha, *ACS Omega* **2021**, *6*, 16847.
28. H. Korbekandi, S. Iravani, S. Abbasi, *Crit. Rev. Biotechnol.* **2009**, *29*, 279.
29. C. A. Foss Jr, G. L. Hornyak, J. A. Stockert, C. R. Martin, *J. Phys. Chem.* **1992**, *96*, 7497.
30. S.-S. Chang, C.-W. Shih, C.-D. Chen, W.-C. Lai, C. R. C. Wang, *Langmuir* **1999**, *15*, 701.
31. J. Pérez-Juste, I. Pastoriza-Santos, L. M. Liz-Marzán, P. Mulvaney, *Coord. Chem. Rev.* **2005**, *249*, 1870.
32. L. Scarabelli, A. Sánchez-Iglesias, J. Pérez-Juste, L. M. Liz-Marzán, *J. Phys. Chem. Lett.* **2015**, *6*, 4270.
33. M.-Z. Wei, T.-S. Deng, Q. Zhang, Z. Cheng, S. Li, *ACS Omega* **2021**, *6*, 9188.
34. F. Liebig, R. M. Sarhan, M. Sander, W. Koopman, R. Schuetz, M. Bargheer, J. Koetz, *ACS Appl. Mater. Interfaces* **2017**, *9*, 20247.
35. L. Scarabelli, M. Coronado-Puchau, J. J. Giner-Casares, J. Langer, L. M. Liz-Marzán, *ACS Nano* **2014**, *8*, 5833.
36. C. Kuttner, M. Mayer, M. Dulle, A. Moscoso, J. M. López-Romero, S. Förster, A. Fery, J. Pérez-Juste, R. Contreras-Cáceres, *ACS Appl. Mater. Interfaces* **2018**, *10*, 11152.
37. J.-E. Park, Y. Lee, J.-M. Nam, *Nano Lett.* **2018**, *18*, 6475.
38. R. Omar, A. En Naciri, S. Jradi, Y. Battie, J. Toufaily, H. Mortada, S. Akil, *J. Mater. Chem. C* **2017**, *5*, 10813.
39. X. Wen, L. Zhang, J. Tian, *J. Phys. Conf. Ser.* **2021**, *1906*, 012023.
40. P. Senthil Kumar, I. Pastoriza-Santos, B. Rodríguez-González, F. Javier García de Abajo, L. M. Liz-Marzán, *Nanotechnology* **2008**, *19*, 015606.
41. I. B. Becerril-Castro, I. Calderon, N. Pazos-Perez, L. Guerrini, F. Schulz, N. Feliu, I. Chakraborty, V. Giannini, W. J. Parak, R. A. Alvarez-Puebla, *Anal. Sens.* **2022**, *2*, e202200005.
42. D. W. Mulder, M. M. Phiri, A. Jordaan, B. C. Vorster, *R. Soc. Open Sci.* **2022**, *6*, 190160.
43. F. Liebig, R. Henning, R. M. Sarhan, C. Prietzel, C. N. Z. Schmitt, M. Bargheer, J. Koetz, *RSC Adv.* **2019**, *9*, 23633.
44. J. Zhu, F. Zhang, J.-J. Li, J.-W. Zhao, *Sens. Actuators B Chem.* **2013**, *183*, 556.
45. S.-J. Ding, J. Zhu, *Appl. Surf. Sci.* **2015**, *357*, 487.
46. A. M. Fales, H. Yuan, T. Vo-Dinh, *J. Phys. Chem. C* **2014**, *118*, 3708.
47. M. S. Zalaffi, L. Litti, P. Canton, M. Meneghetti, L. M. Moretto, P. Ugo, *Nano Express* **2020**, *1*, 020006.
48. P. Wu, L.-B. Zhong, Q. Liu, X. Zhou, Y.-M. Zheng, *Nanoscale* **2019**, *11*, 12829.
49. C. Matricardi, C. Hanske, J. L. Garcia-Pomar, J. Langer, A. Mihi, L. M. Liz-Marzán, *ACS Nano* **2018**, *12*, 8531.
50. Y. Hu, H. Cheng, X. Zhao, J. Wu, F. Muhammad, S. Lin, J. He, L. Zhou, C. Zhang, Y. Deng, P. Wang, Z. Zhou, S. Nie, H. Wei, *ACS Nano* **2017**, *11*, 5558.
51. D. L. Jeanmaire, R. P. Van Duyne, *J. Electroanal. Chem. Interfacial Electrochem.* **1977**, *84*, 1.
52. S. He, M. W. C. Kang, F. J. Khan, E. K. M. Tan, M. A. Reyes, J. C. Y. Kah, *J. Opt.* **2015**, 17.
53. G. Lu, T. Z. Forbes, A. J. Haes, *Analyst* **2016**, *141*, 5137.
54. T. Janči, D. Valinger, J. Gajdoš Kljusurić, L. Mikac, S. Vidaček, M. Ivanda, *Food Chem.* **2017**, *224*, 48.
55. A. Y. F. Mahmoud, C. J. Rusin, M. T. McDermott, *Analyst* **2020**, *145*, 1396.
56. N. Logan, J. Lou-Franco, C. Elliott, C. Cao, *Environ. Sci. Nano* **2021**, *8*, 2718.

57. C. Deriu, A. Bracho, B. McCord, *J. Phys. Chem. C* **2022**, *126*, 2023.
58. W. Ma, M. Sun, L. Xu, L. Wang, H. Kuang, C. Xu, *Chem. Commun.* **2013**, *49*, 4989.
59. C. J. Rusin, M. El Bakkari, R. Du, Y. Boluk, M. T. McDermott, *ACS Appl. Nano Mater*. **2020**, *3*, 6584.
60. M. Fleischmann, P. J. Hendra, A. J. McQuillan, *Chem. Phys. Lett.* **1974**, *26*, 163.
61. J. Zheng, X. Li, R. Gu, T. Lu, *J. Phys. Chem. B* **2002**, *106*, 1019.
62. W. Wang, Y.-F. Huang, D.-Y. Liu, F.-F. Wang, Z.-Q. Tian, D. Zhan, *J. Electroanal. Chem.* **2016**, *779*, 126.
63. M. H. Lin, L. Sun, F. Kong, M. Lin, *Food Control* **2021**, *130*, 108280.
64. F. Zhang, X. Yang, D. Wang, L. Yu, Y. Hu, A. Zhu, C. Zhang, Y. Zheng, T. Yin, Y. Zhang, W. Xie, *J. Raman Spectrosc*. **2022**, *53*, 1227.
65. A. E. Kandjani, M. Mohammadtaheri, A. Thakkar, S. K. Bhargava, V. Bansal, *J. Colloid Interface Sci.* **2014**, *436*, 251.
66. S. M. Tabakman, Z. Chen, H. S. Casalongue, H. Wang, H. Dai, *Small* **2011**, *7*, 499.
67. L. Petti, R. Capasso, M. Rippa, M. Pannico, P. La Manna, G. Peluso, A. Calarco, E. Bobeico, P. Musto, *Vib. Spectrosc.* **2016**, *82*, 22.
68. N. N. Durmanov, R. R. Guliev, A. V Eremenko, I. A. Boginskaya, I. A. Ryzhikov, E. A. Trifonova, E. V Putlyaev, A. N. Mukhin, S. L. Kalnov, M. V Balandina, A. P. Tkachuk, V. A. Gushchin, A. K. Sarychev, A. N. Lagarkov, I. A. Rodionov, A. R. Gabidullin, I. N. Kurochkin, *Sens. Actuators B Chem*. **2018**, *257*, 37.
69. K. K. Y. Wong, X. Liu, *Medchemcomm* **2010**, *1*, 125.
70. S. Galdiero, A. Falanga, M. Vitiello, M. Cantisani, V. Marra, M. Galdiero, *Molecules* **2011**, *16*, 8894.
71. F. Pilaquinga, J. Morey, M. Torres, R. Seqqat, M. de las N Piña, *WIREs Nanomed. Nanobiotechnol.* **2021**, *13*, e1707.
72. F. Le, D. W. Brandl, Y. A. Urzhumov, H. Wang, J. Kundu, N. J. Halas, J. Aizpurua, P. Nordlander, *ACS Nano* **2008**, *2*, 707.
73. H.-Y. Chen, M.-H. Lin, C.-Y. Wang, Y.-M. Chang, S. Gwo, *J. Am. Chem. Soc.* **2015**, *137*, 13698.
74. S.-G. Park, C. Mun, M. Lee, T. Y. Jeon, H.-S. Shim, Y.-J. Lee, J.-D. Kwon, C. S. Kim, D.-H. Kim, *Adv. Mater.* **2015**, *27*, 4290.
75. C. Zhu, G. Meng, P. Zheng, Q. Huang, Z. Li, X. Hu, X. Wang, Z. Huang, F. Li, N. Wu, *Adv. Mater.* **2016**, *28*, 4871.
76. M. Labib, E. H. Sargent, S. O. Kelley, *Chem. Rev.* **2016**, *116*, 9001.
77. L. Ma, H. Wu, Y. Huang, S. Zou, J. Li, Z. Zhang, *ACS Appl. Mater. Interfaces* **2016**, *8*, 27162.
78. W. Yan, L. Yang, J. Chen, Y. Wu, P. Wang, Z. Li, *Adv. Mater.* **2017**, *29*, 1702893.
79. J. Liu, X. Jiang, R. Zhang, Y. Zhang, L. Wu, W. Lu, J. Li, Y. Li, H. Zhang, *Adv. Funct. Mater.* **2019**, *29*, 1807326.
80. X. Wu, X. Fan, Z. Yin, Y. Liu, J. Zhao, Z. Quan, *Chem. Commun.* **2019**, *55*, 7982.
81. L. Zhu, X. Liu, J. Yang, Y. He, Y. Li, *Anal. Chem.* **2020**, *92*, 11981.
82. Z. Li, Y. Song, C. Fan, T. Xu, X. Zhang, *Electroanalysis* **2021**, *33*, 2401.
83. Y.-H. Chang, C. Liu, S. Rouvimov, T. Luo, S.-P. Feng, *Chem. Commun.* **2017**, *53*, 6752.
84. S. P. McDarby, C. J. Wang, M. E. King, M. L. Personick, *J. Am. Chem. Soc.* **2020**, *142*, 21322.
85. G. C. Beaton, A. J. Bottomley, D. Prezgot, A. Ianoul, K. G. Stamplecoskie, *J. Mater. Chem. C* **2020**, *8*, 10755.
86. Z. Li, Y. Luo, Y. Song, Q. Zhu, T. Xu, X. Zhang, *Anal. Chim. Acta* **2022**, *1234*, 340523.
87. J. L. Elechiguerra, J. L. Burt, J. R. Morones, A. Camacho-Bragado, X. Gao, H. H. Lara, M. J. Yacaman, *J. Nanobiotechnol.* **2005**, *3*, 6.
88. L. Sepunaru, B. J. Plowman, S. V Sokolov, N. P. Young, R. G. Compton, *Chem. Sci.* **2016**, *7*, 3892.
89. E. Zavyalova, O. Ambartsumyan, G. Zhdanov, D. Gribanyov, V. Gushchin, A. Tkachuk, E. Rudakova, M. Nikiforova, N. Kuznetsova, L. Popova, B. Verdiev, A. Alatyrev, E. Burtseva, A. Ignatieva, A. Iliukhina, I. Dolzhikova, A. Arutyunyan, A. Gambaryan, V. Kukushkin, *Nanomaterials* **2021**, *11*, 1394.
90. J. Lan, J. Ge, J. Yu, S. Shan, H. Zhou, S. Fan, Q. Zhang, X. Shi, Q. Wang, L. Zhang, X. Wang, *Nature* **2020**, *581*, 215.
91. Y. Zhao, Z. Zhao, Y. Wang, Y. Zhou, Y. Ma, W. Zuo, *bioRxiv.* **2020**, *2020*, 01.26.919985. https://doi.org/10.1101/2020.01.26.919985
92. M. Rozenberg, A. Loewenschuss, Y. Marcus, *Phys. Chem. Chem. Phys.* **2000**, *2*, 2699.
93. K. Tomobe, E. Yamamoto, D. An Kojić, Y. Sato, M. Yasui, K. Yasuoka, **2017**, at <https://www.science.org>.
94. D. Zhang, X. Zhang, R. Ma, S. Deng, X. Wang, X. Wang, X. Zhang, X. Huang, Y. Liu, G. Li, J. Qu, Y. Zhu, J. Li, *Water Res*. **2021**, *200*, 117243.
95. A. Pramanik, Y. Gao, S. Patibandla, D. Mitra, M. G. McCandless, L. A. Fassero, K. Gates, R. Tandon, P. C. Ray, *J. Phys. Chem. Lett.* **2021**, *12*, 2166.
96. Y. Zhang, M. Juhas, C. K. Kwok, *Trends Biotechnol.* **2022**, *41*, 528. https://doi.org/10.1016/j.tibtech.2022.07.012
97. M. J. Bistaffa, S. A. Camacho, W. M. Pazin, C. J. L. Constantino, O. N. Oliveira, P. H. B. Aoki, *Talanta* **2022**, *244*, 123381.
98. J. E. Sanchez, S. A. Jaramillo, E. Settles, J. J. Velazquez Salazar, A. Lehr, J. Gonzalez, C. Rodríguez Aranda, H. R. Navarro-Contreras, M. O. Raniere, M. Harvey, D. M. Wagner, A. Koppisch, R. Kellar, P. Keim, M. Jose Yacaman, *RSC Adv*. **2021**, *11*, 25788.
99. Q. Yu, Y. Wu, T. Kang, J. Choo, *Bull. Korean Chem. Soc.* **2021**, *42*, 1699.
100. Y. Gao, Y. Han, C. Wang, L. Qiang, J. Gao, Y. Wang, H. Liu, L. Han, Y. Zhang, *Anal. Chim. Acta* **2021**, *1154*, 338330.
101. H. Cha, H. Kim, Y. Joung, H. Kang, J. Moon, H. Jang, S. Park, H.-J. Kwon, I.-C. Lee, S. Kim, D. Yong, S.-W. Yoon, S.-G. Park, K. Guk, E.-K. Lim, H. G. Park, J. Choo, J. Jung, T. Kang, *Biosens. Bioelectron.* **2022**, *202*, 114008.
102. D. Antoine, M. Mohammadi, M. Vitt, J. M. Dickie, S. S. Jyoti, M. A. Tilbury, P. A. Johnson, K. E. Wawrousek, J. G. Wall, *ACS Sens.* **2022**, *7*, 866.
103. G. A. Naikoo, F. Arshad, I. U. Hassan, T. Awan, H. Salim, M. Z. Pedram, W. Ahmed, V. Patel, A. S. Karakoti, A. Vinu, *Bioeng. Transl. Med.* **2022**, *7*, e10305.
104. C. J. Toft, R. A. Bourquin, A. E. Sorenson, P. F. Horwood, J. D. Druce, P. M. Schaeffer, *Talanta Open* **2023**, *7*, 100187.
105. Y. Joung, K. Kim, S. Lee, B.-S. Chun, S. Lee, J. Hwang, S. Choi, T. Kang, M.-K. Lee, L. Chen, J. Choo, *ACS Sens.* **2022**, *7*, 3470.
106. G. Seo, G. Lee, M. J. Kim, S.-H. Baek, M. Choi, K. B. Ku, C.-S. Lee, S. Jun, D. Park, H. G. Kim, S.-J. Kim, J.-O. Lee, B. T. Kim, E. C. Park, S. Il Kim, *ACS Nano* **2020**, *14*, 5135.
107. H. C. Ates, A. K. Yetisen, F. Güder, C. Dincer, *Nat. Electron.* **2021**, *4*, 13.
108. D. Yu, V. W.-W. Yam, *J. Am. Chem. Soc.* **2004**, *126*, 13200.

How to cite this article: N. Abu Bakar, N. N. Yusoff, F. S. Nor Azmi, J. G. Shapter, *Aggregate* **2023**, *4*, e339. https://doi.org/10.1002/agt2.339

AUTHOR BIOGRAPHIES

Norhayati Abu Bakar is a research fellow at the Institute of Microengineering and Nanoelectronics, Universiti Kebangsaan Malaysia. She is currently working at the University of Queensland as a postdoctoral research fellow. She received her PhD from Universiti Kebangsaan Malaysia in 2015. She works in the Organic Printed Hybrid Flexible Electronics (OHFEL) group on the detection of organic pollutants in agriculture and the environment and the analysis of biological molecules using homemade optical sensors. Her research areas of interest are the synthesis of nanomaterials and their applications in plasmonic biosensors and surface-enhanced Raman scattering.

Nur Nazhifah Yusoff received a degree in Science physics from Universiti Teknologi MARA (UiTM), Perlis, Malaysia in 2019. She is currently pursuing a Master's degree at the Institute of Microengineering and Nanoelectronics, Universiti Kebangsaan Malaysia. Her research interests include the synthesis of 2D materials and their application in surface-enhanced Raman scattering (SERS).

Farah Shahadah Nor Azmi is a graduate student at the Institute of Microengineering and Nanoelectronics, Universiti Kebangsaan Malaysia. She is currently a member of the Organic Printed Hybrid Flexible Electronics (OHFEL) group, working on nanomaterials and their applications in plasmonic biosensors.

Joseph George Shapter obtained his Ph. D. from the University of Toronto in 1990. In 1996, he moved to Flinders University as a Professor of Nanotechnology. From early 2018 to 2022, he was the Pro Vice-Chancellor (Research Infrastructure) at the University of Queensland and was also a Senior Group Leader at the Australian Institute for Bioengineering and Nanotechnology. In research, our group makes nanomaterials These materials have been used for applications in areas such as sensing and solar cells.